Structure and evolution of the Ivy protein family, unexpected lysozyme inhibitors in Gram-negative bacteria

Chantal Abergel, Vincent Monchois, Deborah Byrne, Sabine Chenivesse, Frédérique Lembo, Jean-Claude Lazzaroni, and Jean-Michel Claverie

PNAS published online Apr 3, 2007;
doi:10.1073/pnas.0611019104

Structure and evolution of the Ivy protein family, unexpected lysozyme inhibitors in Gram-negative bacteria

Chantal Abergel*†, Vincent Monchois*‡, Deborah Byrne*, Sabine Chenivesse*, Frédérique Lembo*, Jean-Claude Lazzaroni§¶, and Jean-Michel Claverie*

*Structural and Genomic Information Laboratory, Centre National de la Recherche Scientifique, Unité Propre de Recherche 2589, Institut de Biologie Structurale et Microbiologie–Institut Fédératif de Recherche 88, Parc Scientifique de Luminy, 163 Avenue de Luminy, Case 934, 13288 Marseille, Cedex 9, France; and §Unité de Microbiologie et Génétique, Unité Mixte de Recherche 5577, Université Claude Bernard Lyon1, Bât 405, F-69622 Villeurbanne Cedex, France

Edited by Janet M. Thornton, European Bioinformatics Institute, Cambridge, United Kingdom, and approved February 20, 2007 (received for review December 12, 2006)

Part of an ancestral bactericidal system, vertebrate C-type lysozyme targets the peptidoglycan moiety of bacterial cell walls. We report the crystal structure of a protein inhibitor of C-type lysozyme, the *Escherichia coli* Ivy protein, alone and in complex with hen egg white lysozyme. Ivy exhibits a novel fold in which a protruding five-residue loop appears essential to its inhibitory effect. This feature guided the identification of Ivy orthologues in other Gram-negative bacteria. The structure of the evolutionary distant *Pseudomonas aeruginosa* Ivy orthologue was also determined in complex with hen egg white lysozyme, and its antilysozyme activity was confirmed. Ivy expression protects porous cell-wall *E. coli* mutants from the lytic effect of lysozyme, suggesting that it is a response against the permeabilizing effects of the innate vertebrate immune system. As such, Ivy acts as a virulence factor for a number of Gram-negative bacteria-infecting vertebrates.

antilysozyme | innate vertebrate immune system

Lysozyme was discovered in 1921 by Sir Alexander Fleming, who was then trying to understand the inhibitory property of his own nasal mucus on the growth of *Staphylococcus* cultures. This discovery stimulated Fleming's search for antimicrobial compounds and probably paved the way for his later discovery of penicillin (1). For the next 80 years, lysozyme continued to play a central role as a model enzyme in many aspects of modern biology (2), including protein chemistry, crystallography, NMR, enzymology, and immunology, as well as in the study of protein folding (3). The classical representative of this widespread enzyme family is the hen egg white lysozyme (HEWL), known as C-type lysozyme. HEWL was the first enzyme to have its structure determined by x-ray crystallography (4). Chicken C-type lysozymes have been characterized in many other animal species, including mammals, reptiles, and invertebrates. The enzymatic specificity of C-type lysozymes, as well as of other distinct types characterized in birds, phages, bacteria, fungi, invertebrates, and plants, is to cleave the β-glycosidic bond between the C-1 of *N*-acetylmuraminic acid and the C-4 of *N*-acetylglucosamine of peptidoglycan, a reticulated polymer forming the rigid layer of bacterial cell walls (5). This enzymatic activity is thought to be at the origin of the antibacterial specificity of lysozyme against Gram-positive bacteria, and to a lesser extent against Gram-negative bacteria, although an alternative mechanism has been proposed (5). In human, C-type lysozyme is present at high concentration (up to 50 $\mu g \cdot ml^{-1}$) in all secretions, including tears and saliva. C-type lysozyme is thought to have evolved from an ancestral metazoan bactericidal defense system (6).

During the course of a systematic survey of *Escherichia coli* genes of unknown functions, we discovered a protein inhibitor of C-type lysozyme, as the product of the *ykfE/ivy* gene (7). Here, we report the *E. coli* Ivy periplasmic protein (Ivyc) crystal structure at 1.6-Å resolution in both isolation and complex with HEWL, and the structure of the orthologous gene product in *Pseudomonas aeruginosa* (Ivyp1), also in complex with HEWL. These structures were used to guide bioinformatics analyses and design directed mutagenesis experiments aimed at exploring the interplay of lysozyme vs. antilysozyme activities in the control of bacterial growth.

Results

Overall Structure of *E. coli* Ivy Protein [Protein Data Bank (PDB) Code 1XS0]. The protein encoded by the *ykfE* gene was expressed and purified in the context of a structural genomics project systematically targeting *E. coli* genes of unknown function. The YkfE protein was serendipitously found to copurify, and then to cocrystallize with HEWL used in the routine bacterial disruption protocol. The YkfE protein was subsequently characterized as a potent and specific inhibitor for C-type lysozyme (7), and the gene name was changed to Ivy (inhibitor of vertebrate lysozyme) to reflect this property. High-resolution crystal structures have been obtained for *E. coli* Ivy (Ivyc) in both isolation and complex with lysozyme [supporting information (SI) Table 1 and Figs. 1 and 2].

Description of the Structure. We previously demonstrated by gel filtration and fluorescence studies that the periplasmic Ivyc homodimer is the physiologically active unit, with a dimerization K_d in the 10^{-9} M range (7). The Ivyc protein crystallized as a dimer. The crystal asymmetric unit contains three molecules corresponding to a noncrystallographic dimer and a monomer. By applying the crystallographic symmetry, this monomer reconstructs the physiological dimer. Each monomer consists of a central β-sheet made of five antiparallel β-strands flanked on the convex side by two short helices (α_1, α_2; six and eight residues, respectively) and, on the

Author contributions: C.A., V.M., and J.-M.C. designed research; C.A., V.M., D.B., S.C., and F.L. performed research; J.-C.L. contributed new reagents/analytic tools; C.A., V.M., and J.-M.C. analyzed data; and C.A. and J.-M.C. wrote the paper.

The authors declare no conflict of interest.

This article is a PNAS Direct Submission.

Freely available online through the PNAS open access option.

Abbreviations: HEWL, hen egg white lysozyme; PDB, Protein Data Bank.

†To whom correspondence should be addressed. E-mail: chantal.abergel@igs.cnrs-mrs.fr.

‡Present address: Protein'eXpert, 15 Rue des Martyrs, 38000 Grenoble, France.

¶Present address: Microbiologie, Adaptation et Pathogénie, Unité Mixte de Recherche, Centre National de la Recherche Scientifique–Université Clande Bernard–Institut National des Sciences Appliquées–Bayer Crop Science, Université Lyon 1, Bat André LWOFF, 10 Rue Raphael Dubois, 69622 Villeurbanne Cedex, France.

This article contains supporting information online at www.pnas.org/cgi/content/full/0611019104/DC1.

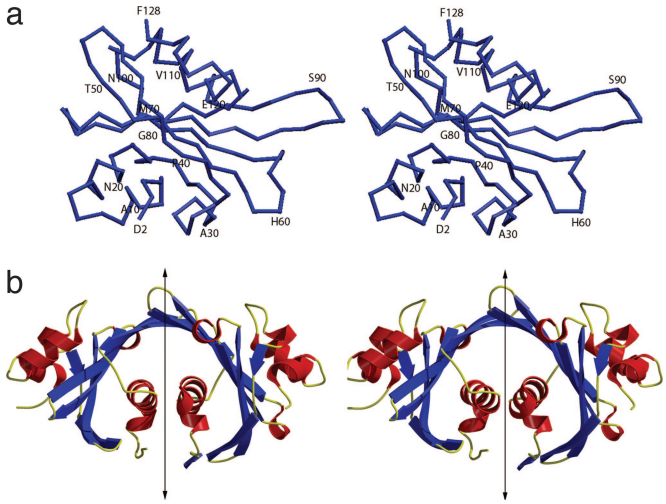

Fig. 1. Stereoviews of the Ivyc structure. (*a*) Cα trace of the Ivyc monomer (residues 2–128). (*b*) Ribbon structure of the Ivyc dimer.

concave side, by an amphipatic helix (α_4; 11 residues) (Fig. 1). We searched for structural homologues of this domain by using the program DALI (8). The best structural match in the PDB is the 306-aa histone acetyltransferase (PDB code 1BOB) from yeast ($Z = 5.2$), with only 9% of identical residues over 89 amino acids and a rmsd of 4.0 Å. However, the topology of the two structures is markedly different, thus making the Ivy structure a novel fold. The dimer structure exhibits a horseshoe-like fold centered on the two antiparallel amphipatic helices (α_4) (Fig. 1*b*). In the crystal, there is 1,605-Å^2 buried surface area between the two monomers related by the crystallographic 2-fold axis (monomer A) and 1,432-Å^2 buried surface area between the two monomers related by the noncrystallographic 2-fold axis (monomers B and C). The rmsd between the three monomers ranges from 0.547 Å (B/C) to 0.865 Å over 122 residues (A/B) based on Cα superimposition. The structure reveals that the dimer involves interactions between backbones and side chains of residues all gathered in the C-terminus part of the molecule in the β6 strand and the α4 and α5 helices (Fig. 2*b*). These residues are conserved in various *E. coli* strains, *Shigella flexneri*, *Klebsiella pneumoniae*, and *Burkholderia cepacia* homologues sequences, suggesting that the Ivy protein is a functional dimer in these bacteria and probably monomeric in the other Ivy-containing bacteria.

Mechanism of Lysozyme Inhibition: The Ivyc–HEWL Complex Structure (PDB Code 1GPQ). The crystal asymmetric unit contains one noncrystallographic homodimer of Ivyc in complex with two molecules of HEWL. There are two types of Ivyc/HEWL interactions: the main interaction involving a 969-Å^2 buried surface area between one Ivyc monomer and one HEWL molecule, and a secondary interaction involving a 552-Å^2 buried surface area between the second Ivyc monomer and the same HEWL molecule, thus creating a 1,340-Å^2 buried surface area between the Ivyc homodimer and

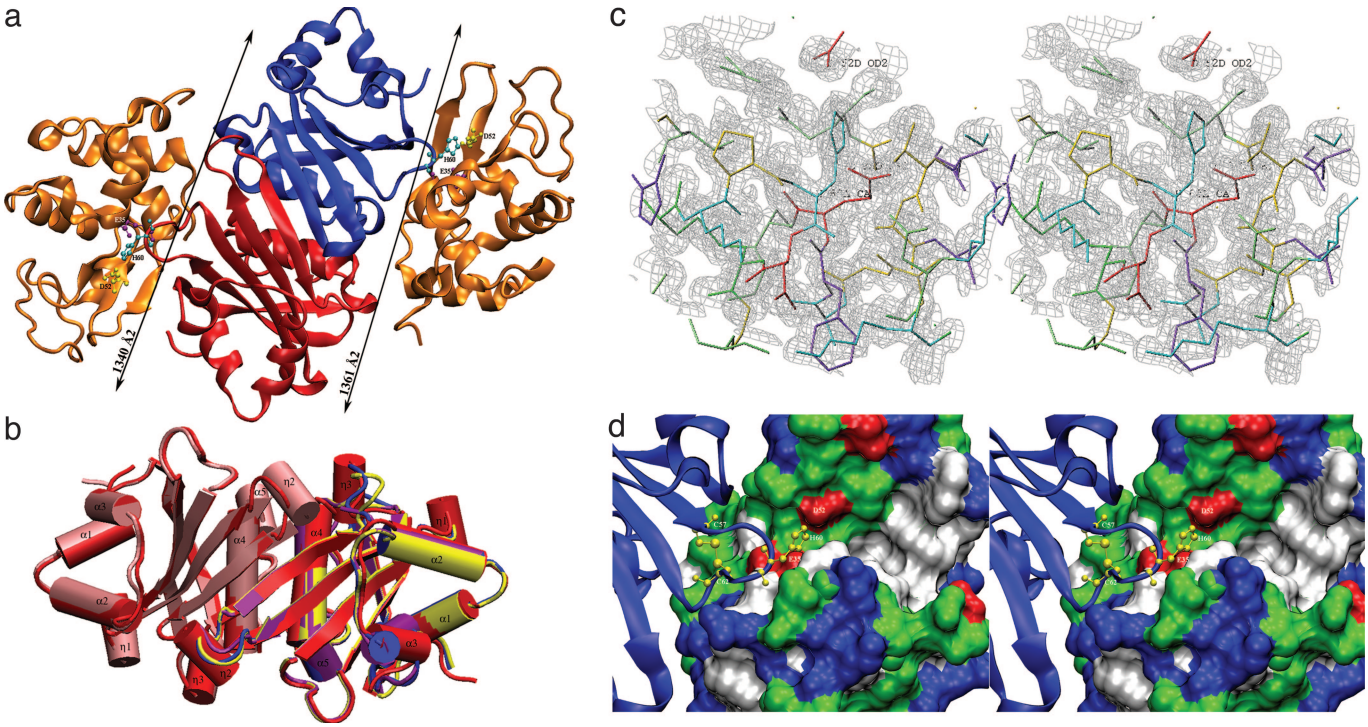

Fig. 2. The Ivyc structure. (*a*) Cartoon representation of the Ivyc–HEWL complex. Monomers of the Ivyc dimer are colored blue and red, and the two lysozyme molecules are colored orange. The Ivyc H60 residues responsible of the HEWL inhibition are represented as light blue balls and sticks. The HEWL D52 residue is colored in yellow, and the E35 is in purple with balls and sticks representation. These two residues are part of the HEWL active site and make hydrogen bonds with the Ivyc H60 residues. The black arrows line up the surface contact area between the Ivyc dimer and each lyzosyme molecule. (*b*) Cartoon representation of the superimposition of the Ivy molecules in the complex structure (red and pink) and the three isolated Ivyc molecules (yellow, blue, purple) superimposed with one Ivyc molecule from the complex (red). Secondary structure elements are marked on the structure. (*c*) Stereoview of the electron density map of the Ivyc protruding loop penetrating the HEWL active site. The two $F_o - F_c$ electronic density map is contoured at 1.0 σ. Residues are colored by types: basic residues in cyan, acidic residues in red, polar residues in light green, hydrophobic residues in yellow, cysteine residues in green, and aromatic residues in purple. Ivyc H60 and HEWL E35 and D52 are labeled. (*d*) Interaction of the Ivyc loop (CKPHDC) with the lysozyme active site. Ivyc is represented as a blue ribbon; H60, C57, and C62 are yellow balls and sticks; and the lysozyme active site as molecular surface is colored according to residue types (acidic, red; polar, green; hydrophobic, white; basic, blue).

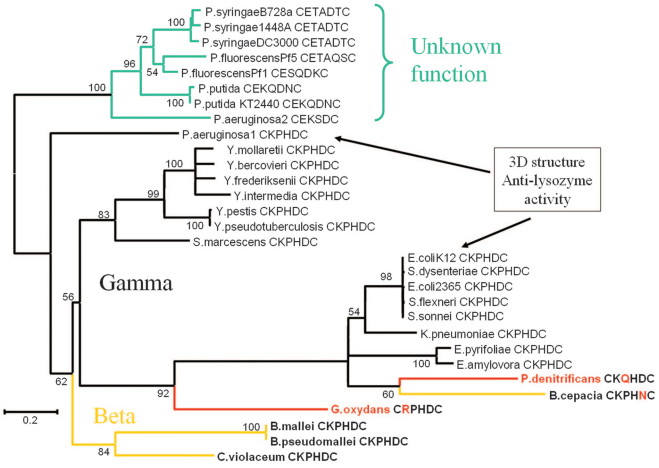

Fig. 3. Phylogenetic analysis of the Ivy protein family. The phylogenetic tree suggests that an ancestor of Ivyc existed in both the gamma and beta divisions (in yellow) but was subsequently lost in some of the gamma (e.g., *Salmonella*) and beta division clades (e.g., most *Neisseriaceae* and *Bordetella*). The anomalous position of the branch leading to the few alpha species (in red) in which Ivy is identified strongly suggests an acquisition by horizontal transfer from *Enterobacteria*, as was probably the case for *B. cepacia* (loss of the *Burkholderia*-derived gene, acquisition from *Enterobacteria*). Ivyc paralogous sequences exhibiting the noncanonical loop motif (in green) appear to have emerged from a duplication within and limited to the *Pseudomonas* clade (followed by the loss of the original Ivyc orthologue, except for *P. aeruginosa*).

the first HEWL molecule (Fig. 2*a*). For the second HEWL monomer, the buried surface area is 1,043 Å^2 for the main interaction and 623 Å^2 for the secondary interaction, leading to a total of 1,361-Å^2 buried surface area between the Ivyc homodimer and the second HEWL molecule.

The structure of the complex confirms the experimental stoechiometry of the interaction between Ivyc and HEWL (7) and immediately suggests the mechanism of lysozyme inhibition by the Ivyc molecule. Through the Ivyc/HEWL complex formation, the lysozyme active site becomes occluded by a loop protruding from the Ivyc molecule (Fig. 2 *c* and *d*). At the center of this loop, a histidine residue (H60) makes hydrogen bonds with two of the three residues responsible for the enzymatic activity of the lysozyme (D52 and E35). The lysozyme molecule complexed with Ivyc does not exhibit any significant structural change (rmsd ≈0.5 Å over 127 residues based on the Cα superimposition of 1HEL with the lysozyme molecules in the crystal). However, one water molecule is excluded from the lysozyme active site and replaced by the histidine of the Ivyc inhibitory loop.

The comparison of the refined structures of Ivyc in isolation or complexed with HEWL (Fig. 2*b* and SI Table 2) reveals a few minor conformational changes. These include the orientation of the small helix (α3) in the three monomers of the free Ivyc form. The orientation observed in molecule A is the closest to the one observed in the Ivyc dimer complexed with HEWL. Three 3_{10}-helices (η1, η2, and η3) seen in the Ivyc/HEWL structure are absent in the three uncomplexed Ivy molecules. More surprisingly, the protruding Ivy loop directly interacting with the lysozyme active site does not exhibit a noticeable conformational change between the two crystal forms. The rigidity of this rather short loop may be explained by the presence of a disulfide bond (C57–C62) and a salt bridge between the lysine residue (K58) next to the first cysteine and the aspartate residue (D61) next to the second cysteine. These structural constraints suggesting a key-lock type of interaction with C-type lysozymes might explain the strict conservation of the loop sequence between a subset of Ivy homologues (Ivyc orthologues) even in distantly related bacteria (Fig. 3 and SI Fig. 5).

Functional Studies: Characterization of ΔIvy *E. coli* Mutants. The central role of the CKPHDC loop in the inhibition was experimentally validated by directed mutagenesis. Amino acid substitutions were performed to assess the influence of some of the key interacting residues as suggested by the structure of the Ivyc/HEWL complex. As expected, we observed a lower inhibitory activity for the histidine (H60) mutants. The most drastic effect (300-fold increase in K_i) was observed when introducing a negatively charged aspartic residue at this position (SI Table 3). This effect is most likely caused by a repulsive interaction with the two acidic residues of the lysozyme active site (D52 and E35). On the other hand, no significant change in the inhibitory activity was observed when introducing a C62 → A62 mutation disrupting the disulfide bridge.

We performed a knockout of the *E. coli ivy* gene to assess the *in vivo* protective effect of the Ivy protein in the presence of lysozyme. The sole *ivy* gene knockout in *E. coli* did not exhibit a phenotype of increased sensitivity to HEWL, thus confirming that, in laboratory conditions, lysozyme does not penetrate the bacterial wall (9). We then constructed a double mutant by introducing a *TolB-pal* deletion to reproduce the "porous cell-wall" phenotype described earlier (10). It was previously shown that *E. coli* Δ*tolB* mutants exhibit a typical phenotype of sensitivity to drugs and detergents, leakiness, and outer membrane vesicles formation (10, 11), because of impaired envelope synthesis. We measured the sensitivity to lysozyme of the Δ*tolB*Δ*ivy* double mutant with reference to the Δ*tolB* mutant (JC864). In laboratory conditions, the Δ*tolB* mutant was found to be sensitive to lysozyme concentrations higher than the one found in secretions (>50 μg·ml^{-1}; SI Fig. 6), thus demonstrating that protein-sized molecules, in addition to small molecules, can penetrate such leaky *E. coli* cells. The Δ*tolB*Δ*ivy* mutant was then tested and found to exhibit a higher sensitivity to HEWL because for physiological concentrations (50 μg·ml^{-1}; Fig. 4*a*) the lysozyme effect on bacterial growth was already visible, supporting the protective role of Ivyc. This protective effect was further confirmed upon overexpression of Ivyc in a Δ*tolB*Δ*ivy* double mutant carrying an isopropyl β-D-thiogalactoside-inducible expression plasmid (Fig. 4*b*) where the Ivy expression was able to restore bacterial growth for lysozyme concentrations up to 500 μg·ml^{-1}. Similar results have been also described in the context of other permeabilizing treatments (9).

The Ivy Protein Family: Phylogenetic Distribution. An exhaustive search for *E. coli* Ivy protein homologues was performed by using all publicly accessible sequence data, including complete bacterial genome sequences and data from ongoing sequencing projects from all major genome sequencing centers (see *Materials and Methods*). All identified Ivy homologue sequences were iteratively used as queries to optimize the detection of more evolutionary distant relatives. A total of 35 distinct Ivy-like sequences were identified (ranging from 100% to <25% sequence identity with *E. coli* K12 Ivy protein). Surprisingly, Ivy homologues are only identified in members of the Proteobacteria (Gram-negative bacteria), and all of them are predicted to be periplasmic (www.cbs.dtu.dk/services/SignalP). On one hand, it may appear logical that Ivy proteins colocalize with the proteoglycan moiety (the lysozyme substrate) within the periplasmic compartment. On the other hand, the proteoglycan network is thought to be physically shielded from the attack of exogeneous enzymes by the Proteobacteria cell wall and is not considered a natural substrate for lysozyme. The presence of a gene encoding a lysozyme inhibitor in Gram-negative rather than Gram-positive bacteria is thus a paradox. The phylogenetic tree of Ivy homologues is presented in Fig. 3, according to the standard Proteobacteria divisions (12): alpha, beta, gamma, delta, and epsilon. As of today, the Ivy protein family is most represented in the gamma and beta divisions, but two Ivy homologues were unambiguously identified in two unrelated species of the alpha division: *Parococcus denitrificans* and *Gluconobacter oxydans*. Within the gamma and beta divisions, Ivy homologues are sporad-

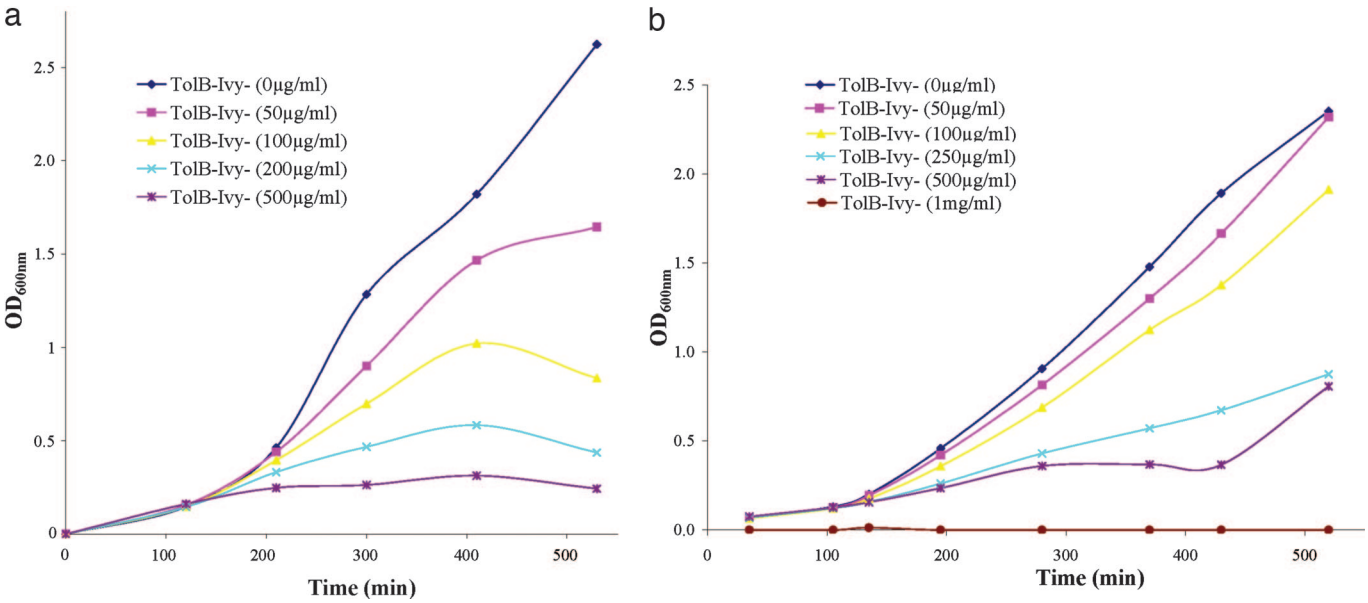

Fig. 4. Effect of increasing concentrations of HEWL on *E. coli* mutants' growth kinetics. (*a*) *E. coli* MG1655 Δ*tolB*Δ*ivy*. (*b*) *E. coli* MG1655 Δ*tolB*Δ*ivy* transformed with the pET26 plasmid expressing the Ivyc protein in the periplasm. For *E. coli* MG1655 Δ*tolB* (JC864) as a control see SI Fig. 6.

ically distributed. For instance, Ivy homologues are present in all *Enterobacteriales*, except in *Salmonella*, but are also found in all sequenced *Pseudomonadaceae*. Similarly in the beta division, Ivy homologues are found in all *Burkholderia*, are identified in a single *Neisseriaceae* species, and are absent from many other sequenced genomes of this division. Such a sporadic distribution of the Ivy protein family denotes a complex underlying evolutionary history made of differential gene losses across clades superimposed with events of horizontal transfers as suggested by detailed phylogenetic analysis (Fig. 3). Except for the alphaproteobacteria, most of the species harboring Ivyc orthologues are pathogens or opportunistic pathogens to human or other vertebrates.

Orthologous vs. Paralogous Ivy Homologues. Most identified members of the Ivy protein family, including the closest homologues to *E. coli* Ivy, exhibit an absolute conservation of the **CKPHDC** subsequence (SI Fig. 5*a*). This motif exactly coincides with the lysozyme inhibitory loop identified in the HEWL/Ivyc complex 3D structure and our functional studies of Ivyc loop mutants (see above). Based on these data, we classified Ivy homologues exhibiting this loop sequence as bona fide orthologues of the *E. coli ivy* gene (i.e., predicted to be lysozyme inhibitors and perform the same function in their respective species). Two additional orthologous sequences contain a nearly exact conservation of the loop with the aspartate residue being replaced by an asparagine residue in the *Burkordelia cepacia* Ivy sequence (48% identity with Ivyc) and the lysine residue being replaced by an arginine residue in the *Gluconobacter oxydans* 621H Ivy sequence (26% sequence identity with Ivyc). The analyses of these mutations in the context of the Ivyc/HEWL complex 3D structure suggest that they both should be compatible with a proper lysozyme/Ivy interaction and thus lysozyme inhibition. The five remaining Ivy homologues exhibiting noncanonical loop sequences were then referred to as *E. coli* Ivy paralogues (i.e., predicted to perform different functions) (SI Fig. 5*b*). Ivy paralogues are only found within species from the *Pseudomonas* genus: *P. aeruginosa*, *P. syringae*, *P. putida*, and *P. fluorescens*, all with related, but different, **CExxDxC** loop sequences. Moreover, *P. aeruginosa* is the sole species exhibiting both an orthologous and a paralogous version of Ivy. The *P. aeruginosa* Ivy orthologous sequence is also the most similar to the *P. aeruginosa* Ivy paralogous sequence, strongly suggesting that a gene duplication leading to the noncanonical loop in Ivy paralogues occurred along the branch leading to the *Pseudomonadaceae*. The absence of Ivy homologues in the close *Acinetobacter* genus might be caused by subsequent gene losses.

Expression and Functional Characterization of *P. aeruginosa* Ivy Homologues. To test our functional predictions about the orthologous versus paralogous Ivy forms, we expressed (see *Materials and Methods*) the product of both *P. aeruginosa* Ivy-related genes. The two proteins called Ivyp1 (orthologue) and Ivyp2 (paralogue) were purified and tested for their inhibitory activity against HEWL. As predicted from their respective loop sequences, the Ivyp1 (CKPHDC) protein was found to inhibit lysozyme activity, whereas Ivyp2 (CEKSDC) did not. The result of the Ivyp1 inhibition of the HEWL activity is presented in SI Fig. 7*a*. As for Ivyc, the inhibition follows a "slow tight binding" mechanism with a Ki_{app} {Ivyp1, HEWL} of ≈25 nM.

Structure of *P. aeruginosa* Ivyp1 (PDB Code 1UUZ). After the demonstration that *P. aeruginosa* Ivyp1 and *E. coli* Ivy exhibited similar antilysozyme activities, we determined the structure of the Ivyp1:HEWL complex to visualize how the inhibitory interaction was preserved despite the remote similarity of these two Ivy protein sequences (30% identical residues; SI Fig. 5*a*). As expected, the structure of Ivyp1 is similar to the Ivyc monomer structure. However, as predicted from the nonconservation of the residues involved in Ivyc dimer formation, *P. aeruginosa* Ivyp1 is a monomer.

Despite this significant difference, the interaction of the two Ivy homologues with the lysozyme molecule is remarkably similar (Fig. 2, SI Fig. 7*b*, and SI Table 4). The Cα rmsd between the Ivyp1 and Ivyc monomers is ≈2.8 Å. We then compared the surfaces of interaction in the two complexes to identify the key residues responsible for the robustness of the Ivy–lysozyme interaction. In both Ivy complexes, the Ivy–HEWL interaction involves the same amount of salt bridges, hydrogen bonds involving side chains, side chains/main chains, and main-chain interactions. However, among the numerous residues involved in the interaction with lysozyme, only three are strictly conserved: the histidine residue (H60 in Ivyc, H62 in Ivyp1) forming both a direct hydrogen bond (E35–OE1) and an indirect hydrogen bond through a water molecule (D52–OD1) within the HEWL active site, one aspartate residue (D61 in Ivyc and

D63 in Ivyp1), and a glutamate residue (E120 in Ivyc and E123 in Ivyp1). We then compared the interaction areas in the two complexes. Because of the dimeric state of the Ivyc molecule, the surface area buried upon Ivyc–HEWL complex formation is larger (≈1,340 Å^2) than for the Ivyp–HEWL complex (≈1,000 Å^2). This difference probably explains the lower inhibitory activity (25-fold decrease) of Ivyp1 compared with Ivyc.

Discussion

We described a protein family with a broad, albeit discontinuous, phylogenetic range. A subset of this family, defined by a highly conserved loop, exhibits a physiologically significant antilysozyme activity, making it a protein inhibitor of lysozyme. The structures of two phylogenetically distant (Fig. 3 and SI Fig. 5) members of the Ivy family, in complex with lysozyme, highlighted the central role of the conserved CKPHDC loop in the enzyme inhibition that occurs via a key-lock type of interaction, in the absence of conformational changes in the Ivy or lysozyme molecules. The Ivy structure corresponds to a new fold, and the protein can be either dimeric as in *E. coli* or monomeric as in *P. aeruginosa*. Comprehensive sequence similarity searches identified a distinct subset of the Ivy family, uniquely found in *Pseudomonas* species and consisting of proteins most likely sharing the same overall structure, but in which the conserved CKPHDC motif is replaced by a more variable sequence still flanked by two conserved cysteines. These divergent Ivy proteins all might function as inhibitors against the same unidentified enzyme or exhibit different activities altogether. Until now, no partners to these *Pseudomonas* Ivy paralogues have been identified to our knowledge.

The complex phylogenetic distribution of the Ivy family lysozyme inhibitor does not lend itself to a simple interpretation. On one hand, antilysozyme Ivy orthologues are found in species from three different proteobacteria division (alpha, beta, and gamma), which would argue in favor of them being a significant and general factor in bacterial fitness. On the other hand, their distribution is highly sporadic within each division and does not clearly correlate with a given ecological niche. In that respect the absence of Ivy homologues in genus *Salmonella* or *Vibrionaceae* is particularly puzzling given their close relationship (and frequent gene exchange) with the Ivy-containing *Enterobacteria*. Even more paradoxical is the fact that the *ivy* genes appear restricted to Gram-negative bacteria, *a priori* not sensitive to lysozyme, and are not found in any Gram-positive bacteria, thought to be the natural target of C-type lysozyme. Our results confirmed that lysozyme had no effect on *E. coli* under laboratory conditions, unless its permeability was artificially increased by introducing a membrane defect, such as in TolB$^-$ mutants. Only under such conditions the expression of *ivy* exhibited a protective effect on the bacterial growth (Fig. 4). Similar circumstances might actually be encountered in the natural environment of Gram-negative bacteria. The innate vertebrate immune system, increasingly recognized as the first line of defense against bacterial infection, produces a number of proteins highly toxic to Gram-negative but not to Gram-positive bacteria (13–17). In synergy, these protective agents (*i*) make pores in the membrane of the pathogen through proteases (e.g., perforins, defensins, bacterial permeability-increasing proteins), (*ii*) opsonize bacteria through serum proteins (e.g., lipopolysaccharide-binding protein, lysozyme), and (*iii*) chemoattract leukocytes. In turn, Gram-negative bacteria have evolved protective mechanisms, such as ecotins, a family of periplasmic proteins inhibiting serine proteases, including the permeabilizing neutrophil elastase (15). The Ivy protein could play a similar role against lysozyme, whereas the Ivy paralogue might inhibit another of the many microbicidal agents present in human nasal and salivatory secretions (18) such as PLUNC proteins, ubiquitous in vertebrate genomes, and known to be active against *P. aeruginosa* (19). Interestingly, the mechanism of Ivy inhibition is similar to the one observed for ecotin against serine proteases, in a substrate-like fashion, through a critical protruding loop (15).

Along the same line, *ivy* gene products secreted by Gram-negative bacteria might also be protective for themselves and neighboring Gram-positive bacteria in natural situations, such as in biofilm (where *Pseudomonas* are predominant) or other symbiotic, for instance intestinal, populations (where *Enterobacteria* abound) (20). Finally, both Ivy and ecotin are part of the 25 genes significantly up-regulated by higher concentrations of acetyl phosphate known to promote the free living state where bacteria are more sensitive to the vertebrate innate immune system (15, 20). Indeed more work is needed to identify the physiological function of Ivy genes that might lead to a reappraisal of the physiological role of C-type lysozyme and related enzymes in the control of opportunistic bacterial infections.

Materials and Methods

Cloning, expression and purification of the Ivyc (7, 21), Ivyp1, and Ivyp2 proteins and the crystallization conditions of the Ivy/HEWL complexes are described in *SI Text*.

Data Collection and Processing. ***Ivyc.*** To use the MAD method (22) to solve the Ivyc structure, a three-wavelength data set was collected at the European Synchrotron Radiation Facility (Grenoble, France) radiation synchrotron facility (BM30A) on a selenomethionine-substituted Ivyc crystal flash-frozen to 105 K. A 1.58-Å resolution data set was also collected on the same crystal at a wavelength of 0.9793 Å (SI Table 1). The crystal lattice was originally misinterpreted as trigonal $P3_1$ with two molecules per asymmetric unit (21) and subsequently reinterpreted as monoclinic, C2, with unit cell parameters $a = 81.34$, $b = 46.96$, $c = 88.04$, and $\beta = 89.95$. There are three molecules per asymmetric unit related by a "frustrated" $P3_121$ crystallographic symmetry (*SI Text*).

Ivyc/HEWL complex. One crystal of Ivyc/HEWL complex flash-frozen to 105 K was collected at the European Synchrotron Radiation Facility (BM30A) at a wavelength of 0.9798 Å. The crystals belong to the monoclinic space group $P2_1$ with unit cell parameters $a = 55.49$ Å, $b = 59.56$ Å, $c = 69.20$ Å, and $\beta = 95.39$. The packing density for two molecules of complex in the asymmetric unit of these crystals (volume 227,694 Å^3) is 2 Å^3·Da^{-1}, indicating an approximate solvent content of 38% (23). Statistics of the 1.6-Å resolution data set are presented in SI Table 1.

Ivyp1/HEWL complex. One crystal of Ivyp1/HEWL complex flash-frozen to 105 K was collected at the European Synchrotron Radiation Facility (ID14EH2) at a wavelength of 0.933 Å. The crystals belong to the monoclinic space group $P2_1$ with unit cell parameters $a = 52.35$ Å, $b = 60.76$ Å, $c = 78.24$ Å, and $\beta = 102.29$. The packing density for two molecules of complex in the asymmetric unit (volume 243,158 Å^3) is 2.14 Å^3·Da^{-1}, corresponding to a 42.5% solvent content (23). Statistics of the 1.8-Å resolution data set are presented in SI Table 1.

Structure Determination and Refinement. ***Ivyc and Ivyc/HEWL.*** Phase determination was performed by using the SOLVE program (24). Phases were calculated on the three wavelengths in the 20- to 2.58-Å resolution range, and a single solution was found with seven sites and a mean figure of merit of 0.85 for all of the data between 20 and 2.58 Å. The phases obtained were improved by using solvent-flattening and histogram-matching techniques as implemented in the DM program (25), and the electron-density maps were used to construct the main chain of the molecules by using TURBO-FRODO (26). Interestingly, the pseudo symmetry was so strong that it was possible to build most of the structure in the $P3_1$ space group except for α_3, η_2, η_3, which could only be refined in the proper space group (*SI Text*). Preliminary refinement was performed with CNS (27) between 20 and 1.58 Å.

The initial phasing of the Ivyc/HEWL complex was then carried out by molecular replacement using AMoRe software (28). Patter-

son rotation and translation search were carried out by using the HEWL coordinates (PDB code 1HEL) and the polyalanine trace of the initial construction (190 of the 270 aa) of the selenomethionine-substituted Ivyc homodimer previously solved by MAD method in the $P3_1$ space group. The best solution of the translation function search corresponding to two HEWL molecules and the Ivyc homodimer partial structure gave a correlation factor of 43% and an R factor of 44%. Refinement was performed with CNS (27) between 20 and 1.6 Å. The final R_{work} and R_{free} were 18.1 and 21.1, respectively. The model includes 519 residues and 635 water molecules (PDB code 1GPQ; SI Table 1). We then came back to the free form of the Ivyc structure to compare it with the Ivyc/HEWL complex structure. Molecular replacement using the refined homodimer Ivyc structure was thus performed on the Ivyc uncomplexed crystal form reprocessed in the C2 space group, and the structure was refined by using CNS and 20- and 1.58-Å data. The final model corresponds to 389 residues and 302 water molecules with R_{work} of 22.5% and R_{free} of 26.0 (SI Table 1) (PDB code 1XS0).

Ivyp1/HEWL. The structure of the Ivyp/Hewl complex was solved by molecular replacement using AMoRe software (28), the HEWL structure (PDB code 1HEL) and one monomer of the Ivyc structure (PDB code 1GPQ). The best solution of the translation function search corresponding to two HEWL molecules and two Ivyc monomers gave a correlation factor of 32% and an R factor of 48%. Refinement was performed by using CNS (27) between 20 and 1.8 Å. After refinement, the final R_{work} and R_{free} were 21.3 and 25.0, respectively (SI Table 1). The model includes 532 residues and 386 water molecules (PDB code 1UUZ).

Figs. 1*a* and 2 *a*, *b*, and *d* were generated with the VMD program (29). Fig. 1*b* was generated with MOLSCRIPT (30), and Fig. 2*c* was generated with TURBO-FRODO (26).

Inhibition Activity Measurements. HEWL activity assay and inhibition studies were performed as described (7) (*SI Text*). HEWL (70 nM) was preincubated with Ivyp1 (0–200 nM) at room temperature for 15 min before the addition of the *Micrococcus lysodeikticus* substrate (0.125 mg·ml^{-1}). Ivyp1 K_i value was determined according to the slow tight binding competitive inhibition model (with no conformational change) (31, 32). We used the Morrison's quadratic equation as follows:

$$(V_{Ivyp1}/V_0)^2 + (V_{Ivyp1}/V_0) \times (It/Et + Ki/Et - 1) - K_i/Et = 0, \quad [1]$$

where K_i is the apparent dissociation constant, Et, the total enzyme (HEWL) concentration, It the total inhibitor (Ivyp1) concentration, V_{Ivyp1}, the inhibited velocity for a given concentration of Ivyp1, and V_0 the velocity in absence of inhibitor.

The K_i value was determined by fitting the experimental data onto the V_{Ivyp1}/V_0 theoretical curves computed from Eq. **1** (SI Fig. 7*a*).

Knockout Constructions. Two constructions were produced to assay the effect of the Ivyc gene knockout on the *E. coli* growth in the presence of lysozyme: ΔIvy and ΔIvyΔTolB (*SI Text*).

Sensitivity to C-Type Lysozyme. *E. coli* mutants sensitivity to lysozyme was measured on 4-ml deepwell cultures at 25°C in LB plus tetracycline (ΔTolB resistance) or LB plus tetracycline plus kanamycin (ΔTolBΔIvy resistance) media inoculated with 200 μl of bacterial cells at a 0.5 OD_{600}. Increasing concentrations (50 μg/ml to 1 mg/ml) of HEWL were added to the growth media, and cell growth was monitored overtime by following their OD absorbance at 600 nm for the two mutants and the ΔTolBΔIvy mutant transformed by the empty pET26 vector as control and the pET26 vector carrying the Ivyc gene used for periplasmic expression of the Ivyc protein. When OD_{600} reached 0.5 Ivyc expression was induced by adding 0.5 mM isopropyl β-D-thiogalactoside.

Phylogenetic Analysis of the Ivy Protein Family. Ivy protein sequences were aligned with 3D-coffee (33) by using the PDB files 1GPQB and 1UUZB as structural references. The neighbor-joining phylogeny was computed with Mega3 (34) (option: pairwise deletion, and JTT amino acid substitution model), and bootstrap values were computed from 250 replications. Branches with bootstrap values <50% were collapsed. The tree was rooted on the branch separating the Ivyc orthologous sequences (harboring the conserved antilysozyme CKPHDC motif) from the Ivyc paralogous sequences harboring a different loop (and of unknown function).

We thank Dr. Jorge Navaza and Dr. Hiroyuki Ogata for helpful discussion, Pr. Alain Filloux (Centre National de la Recherche Scientifique) for the *P. aeruginosa* PAO1 genomic DNA, Dr. Michel Roth for expert help on the BM30A beamline at the European Synchrotron Radiation Facility, and Marseille-Nice Génopole for the use of the Proteomic and Bioinformatics platforms. This study was supported by the Centre National de la Recherche Scientifique, French Ministry of Industry Grant 4906088, and the French National Génopole Network.

1. MacFarlane G (1985) *Alexander Fleming: The Man and the Myth* (Oxford Univ Press, Oxford, UK).
2. Prager EM, Jollès P (1996) *Animal Lysozymes c and g: An Overview* (Birkhäuser, Basel, Switzerland).
3. Matagne A, Dobson CM (1998) *Cell Mol Life Sci* 54:363–371.
4. Blake CC, Koenig DF, Mair GA, North AC, Phillips DC, Sarma VR (1965) *Nature* 206:757–761.
5. Holtje JV (1996) *Exs* 75:105–110.
6. Mallo GV, Kurz CL, Couillault C, Pujol N, Granjeaud S, Kohara Y, Ewbank JJ (2002) *Curr Biol* 12:1209–1214.
7. Monchois V, Abergel C, Sturgis J, Jeudy S, Claverie JM (2001) *J Biol Chem* 276:18437–18441.
8. Holm L, Sander C (1995) *Trends Biochem Sci* 20:478–480.
9. Deckers D, Masschalck B, Aertsen A, Callewaert L, Van Tiggelen CG, Atanassova M, Michiels CW (2004) *Cell Mol Life Sci* 61:1229–1237.
10. Bernadac A, Gavioli M, Lazzaroni JC, Raina S, Lloubes R (1998) *J Bacteriol* 180:4872–4878.
11. Lazzaroni JC, Portalier R (1992) *Mol Microbiol* 6:735–742.
12. Gupta RS (2000) *FEMS Microbiol Rev* 24:367–402.
13. Bingle CD, Gorr SU (2004) *Int J Biochem Cell Biol* 36:2144–2152.
14. Canny G, Levy O, Furuta GT, Narravula-Alipati S, Sisson RB, Serhan CN, Colgan SP (2002) *Proc Natl Acad Sci USA* 99:3902–3907.
15. Eggers CT, Murray IA, Delmar VA, Day AG, Craik CS (2004) *Biochem J* 379:107–118.
16. Levy O, Canny G, Serhan CN, Colgan SP (2003) *Biochem Soc Trans* 31:795–800.
17. Canny G, Cario E, Lennartsson A, Gullberg U, Brennan C, Levy O, Colgan SP (2006) *Am J Physiol* 290:G557–G567.
18. Bingle CD, Craven CJ (2002) *Hum Mol Genet* 11:937–943.
19. Geetha C, Venkatesh SG, Dunn BH, Gorr SU (2003) *Biochem Soc Trans* 31:815–818.
20. Wolfe AJ, Chang DE, Walker JD, Seitz-Partridge JE, Vidaurri MD, Lange CF, Pruss BM, Henk MC, Larkin JC, Conway T (2003) *Mol Microbiol* 48:977–988.
21. Abergel C, Monchois V, Chenivesse S, Jeudy S, Claverie JM (2000) *Acta Crystallogr D* 56:1694–1695.
22. Hendrickson WA, Horton JR, LeMaster DM (1990) *EMBO J* 9:1665–1672.
23. Matthews BW (1968) *J Mol Biol* 33:491–497.
24. Terwilliger TC, Berendzen J (1999) *Acta Crystallogr D* 55:849–861.
25. Cowtan K (1994) *Joint CCP4 ESF-EACBM Newsl Protein Crystallogr* 31:34–38.
26. Roussel A, Cambillau C (1991) *The TURBO-FRODO Graphics Package* (Silicon Graphics, Mountain View, CA).
27. Brunger AT, Adams PD, Clore GM, DeLano WL, Gros P, Grosse-Kunstleve RW, Jiang JS, Kuszewski J, Nilges M, Pannu NS, *et al.* (1998) *Acta Crystallogr D* 54:905–921.
28. Navaza J (2001) *Acta Crystallogr D* 57:1367–1372.
29. Humphrey W, Dalke A, Schulten K (1996) *J Mol Graphics* 14:33–38.
30. Kraulis PJ (1991) *J Appl Crystallogr* 24:946–950.
31. Morrison JF, Walsh CT (1988) *Adv Enzymol Relat Areas Mol Biol* 61:201–301.
32. Morrison JF (1969) *Biochim Biophys Acta* 185:269–286.
33. Poirot O, Suhre K, Abergel C, O'Toole E, Notredame C (2004) *Nucleic Acids Res* 32:W37–W40.
34. Kumar S, Tamura K, Nei M (2004) *Brief Bioinform* 5:150–163.